



The AMPK-PP2A axis in insect fat body is activated by 20-hydroxyecdysone to antagonize insulin/IGF signaling and restrict growth rate

Dongwei Yuan^{a,b,c,1}, Shun Zhou^{b,c,1}, Suning Liu^{a,1} , Kang Li^a, Haigang Zhao^{a,b,c}, Shihui Long^a, Hanhan Liu^{b,c}, Yongfang Xie^d , Yunlin Su^e, Fengwei Yu^f , and Sheng Li^{a,b,2}

^aGuangdong Provincial Key Laboratory of Insect Developmental Biology and Applied Technology, Institute of Insect Science and Technology & School of Life Sciences, South China Normal University, 510631 Guangzhou, China; ^bKey Laboratory of Developmental and Evolutionary Biology, Institute of Plant Physiology and Ecology, Shanghai Institutes for Biological Sciences, Chinese Academy of Sciences, 200032 Shanghai, China; ^cUniversity of Chinese Academy of Sciences, 100049 Beijing, China; ^dBioinformatic College, Chongqing University of Posts and Telecommunications, 400065 Chongqing, China; ^eKey laboratory of South China Agricultural Plant Molecular Analysis and Genetic Improvement, South China Botanical Garden, Chinese Academy of Science, 510650 Guangzhou, China; and ^fTemasek Life Sciences Laboratory and Department of Biological Sciences, Research Link, National University of Singapore, 117604, Singapore

Edited by David L. Denlinger, The Ohio State University, Columbus, OH, and approved March 17, 2020 (received for review January 21, 2020)

In insects, 20-hydroxyecdysone (20E) limits the growth period by triggering developmental transitions; 20E also modulates the growth rate by antagonizing insulin/insulin-like growth factor signaling (IIS). Previous work has shown that 20E cross-talks with IIS, but the underlying molecular mechanisms are not fully understood. Here we found that, in both the silkworm *Bombyx mori* and the fruit fly *Drosophila melanogaster*, 20E antagonized IIS through the AMP-activated protein kinase (AMPK)-protein phosphatase 2A (PP2A) axis in the fat body and suppressed the growth rate. During *Bombyx* larval molt or *Drosophila* pupariation, high levels of 20E activate AMPK, a molecular sensor that maintains energy homeostasis in the insect fat body. In turn, AMPK activates PP2A, which further dephosphorylates insulin receptor and protein kinase B (AKT), thus inhibiting IIS. Activation of the AMPK-PP2A axis and inhibition of IIS in the *Drosophila* fat body reduced food consumption, resulting in the restriction of growth rate and body weight. Overall, our study revealed an important mechanism by which 20E antagonizes IIS in the insect fat body to restrict the larval growth rate, thereby expanding our understanding of the comprehensive regulatory mechanisms of final body size in animals.

fat body | 20-hydroxyecdysone | AMPK-PP2A axis | insulin/IGF signaling | growth rate

The final body size in animals is a fundamental feature that influences many traits, such as fitness, mobility, predation, and competition. In animals undergoing defined growth, the final body size is gradually attained at a relatively steady level during development, but the mechanism underlying this process remains mostly unknown (1, 2). By regulating the growth rate and growth period, respectively, insulin/insulin-like growth factor (IGF) signaling (IIS) and the steroid hormone 20-hydroxyecdysone (20E) are considered the two major factors determining the final body size in insects (3–5). IIS and nutrition coordinate with the intrinsic growth program to regulate the growth rate. Insulin/IGF is mainly synthesized by insulin-producing neurons and secreted to hemolymph upon stimulation by nutrients. The binding of insulin/IGF to the insulin receptor (InR) activates the intrinsic tyrosine kinase activity of its receptor, which activates a downstream signaling cascade, including phosphatidylinositol-4,5-bisphosphate 3-kinase (PI3K), protein kinase B (AKT), and the two main downstream targets of IIS: That is, the target of rapamycin complex 1 (TORC1) and the FOXO transcription factor (6). Meanwhile, 20E signaling triggers developmental transitions and, therefore, controls the growth period and developmental timing. The binding of 20E to its nuclear receptor complex (EcR-USP) triggers a transcriptional cascade that induces molting and metamorphosis (7).

In addition to controlling the growth period, 20E modulates the growth rate by antagonizing IIS in the fat body (8–11). The insect fat body is the major organ of energy storage and nutrient mobilization, and moreover, it plays a critical role in the integration of hormonal and nutritional signals that regulate autophagy and the larval growth rate (12–14). In general, autophagy is induced by the reductions in cell growth, which are caused by nutrient deprivation or other stresses (15). IIS and 20E oppositely regulate fat body autophagy in both the fruit fly *Drosophila melanogaster* and the silkworm *Bombyx mori*. IIS-activated TORC1 prevents starvation-induced autophagy, while 20E signaling induces autophagy by suppressing IIS during metamorphosis (8, 16–19). Meanwhile, 20E signaling impedes IIS, which increases the growth rate by activating TORC1 and inhibiting FOXO, thus restricting the final body size in insects. As the center molecule of energy response, TORC1 promotes the larval growth rate partially by repressing autophagy in *Drosophila* (8, 9, 20, 21). Meanwhile, TORC1 promotes protein synthesis, cell-cycle progression and, thus, cell growth by activating S6K and inhibiting 4EBP (22). The FOXO transcription factors are inactivated by IIS via the translocation from nucleus

Significance

Final body size determination in animals remains a long-standing puzzle in the field of developmental biology. In insects, insulin/insulin-like growth factor signaling (IIS) and the steroid hormone 20-hydroxyecdysone (20E) are mainly responsible for the growth rate and growth period, respectively, and consequently the final body size. Here, we report that 20E activates AMPK by up-regulating its gene expression and inducing sugar starvation. In turn, AMPK activates protein phosphatase 2A, which further dephosphorylates and inactivates key components in IIS in the fat body, and eventually suppresses the larval growth rate. These data answer the question of how 20E antagonizes IIS and modulates growth rate.

Author contributions: D.Y., S.Z., S. Liu, and S. Li designed research; D.Y., S.Z., S. Liu, K.L., H.Z., S. Long, H.L., and Y.X. performed research; F.Y. contributed new reagents/analytical tools; D.Y., S.Z., S. Liu, and S. Li analyzed data; and D.Y., S.Z., S. Liu, Y.S., F.Y., and S. Li wrote the paper.

The authors declare no competing interest.

This article is a PNAS Direct Submission.

Published under the PNAS license.

¹D.Y., S.Z., and S. Liu contributed equally to this work.

²To whom correspondence may be addressed. Email: lisheng@scnu.edu.cn.

This article contains supporting information online at <https://www.pnas.org/lookup/suppl/doi:10.1073/pnas.2000963117/-DCSupplemental>.

First published April 10, 2020.

to cytoplasm (23). In *Drosophila*, FOXO regulates nearly 28% of the nutrient-regulated genes (24). In *Bombyx* and other lepidopteran species, 20E activates FOXO to promote lipolysis and proteolysis during insect molting to suppress cell growth (25, 26). There were two reports about the molecular mechanism of how 20E cross-talks with IIS. In the *Drosophila* fat body, 20E signaling represses the expression of a microRNA, miR-8 (11). This microRNA inhibits the expression of *u-shaped* (*ush*), which acts as an inhibitor of PI3K and thus IIS (27). In addition, 20E might regulate insulin production and secretion in the brain and thus IIS (28). Nevertheless, the underlying molecular mechanisms by which the steroid hormone 20E antagonizes the receptor tyrosine kinase pathway IIS are still not well understood.

AMP-activated protein kinase (AMPK), which consists of three subunits (AMPK α , AMPK β , and AMPK γ) is a molecular sensor that plays a vital role in the maintenance of energy homeostasis at both the cellular and organismal levels (29, 30). In response to metabolic stress, the cellular AMP/ATP ratio increases, leading to the activation of AMPK, which restores energy homeostasis by turning on catabolic pathways and turning off ATP-consuming pathways (31–34). In addition to its role in energy metabolism, AMPK also plays important roles in animal development, tissue growth, and autophagy. Regarding its role in animal development, mutations in α - or β -subunits of AMPK cause death in *Drosophila* at the pupal stage (35–37). In terms of tissue growth, AMPK acts as a tumor suppressor that represses the excessive proliferation of cancer cells in mammals (38); tissue-specific (eyes and wings) overexpression of the upstream AMPK activating kinase LKB1 in *Drosophila* shrinks the sizes of these organs (39). In respect to autophagy, AMPK promotes autophagy in mammals in the following two ways: 1) By directly activating Ulk1, which is a homolog of ATG1 (31, 40); and 2) by inhibiting mTORC1 through phosphorylating raptor, which is a key component of TORC1 (41). In a genetic screen, AMPK γ was revealed to play a role in 20E-induced autophagy in the *Drosophila* fat body (36).

Interestingly, AMPK and IIS might reciprocally antagonize each other. In mammals, AKT suppresses AMPK activity by decreasing the cellular AMP/ATP ratio or through the phosphorylation Ser485 of the AMPK α 1 subunit and Ser491 of the AMPK α 2 subunit (42–44), while AMPK inhibits AKT activity by dephosphorylating AKT through protein phosphatase 2A (PP2A) (45, 46). In *Caenorhabditis elegans*, PP2A also interacts with DAF-18 (PTEN) and AMPK (47). Additionally, PP2A might suppress AMPK activation by dephosphorylating Thr172 of AMPK α -subunits in both mammals and nematode (48–50). However, it remains completely unknown how AMPK and PP2A are involved in the mutual antagonism between 20E and IIS in the control of body size in insects.

In this study, we first discovered that AMPK activity was positively correlated with 20E signaling in the fat body tissues during *Bombyx* larval molting and *Drosophila* pupariation, while IIS was negatively correlated with 20E signaling. Second, we unraveled the following mechanism underlying the antagonism of IIS by 20E in the fat body: AMPK acts through PP2A to inhibit IIS, and 20E relies on the AMPK-PP2A axis to antagonize IIS. Finally, activation of the AMPK-PP2A axis and inhibition of IIS in the *Drosophila* fat body reduced food consumption, resulting in the restriction of growth rate and body weight. These data contribute to our understanding of how 20E antagonizes IIS and modulates the insect growth rate.

Results

AMPK Inhibits IIS in *Bombyx*. To understand the correlation between AMPK activity and IIS in the *Bombyx* fat body, we first examined the developmental profiles of the phosphorylation levels of AMPK α at T172 (reflecting AMPK activity), InR at Y1135/1136 (reflecting IIS), and 4EBP at T37/46 (reflecting

TORC1 activity) in the *Bombyx* fat body from the early fourth instar to the middle fifth instar. Western blot analysis revealed that the AMPK α phosphorylation level was low during the feeding stages in both larval instars but greatly increased during the fourth larval molting (4M) and day 1 of the fifth instar (L5D1) (Fig. 1A). In contrast, the phosphorylation levels of 4EBP and InR were high during the larval feeding stages but decreased at ~4M, when the decrease of 4EBP phosphorylation was more significant (Fig. 1A). In addition, using immunohistochemistry, we previously showed that FOXO nuclear localization is abundant at 4M but nearly undetectable during the larval feeding stages (25). Thus, according to the developmental profiles, a negative correlation between AMPK activity and IIS occurred in the fat body at ~4M. Interestingly, the expression level of the AMPK α protein exhibited a developmental profile that was similar to that of AMPK α phosphorylation with high protein levels at 4M and L5D1 (Fig. 1A). Subsequently, we investigated the developmental profiles of the mRNA levels of AMPK α , AMPK β , and AMPK γ in the *Bombyx* fat body. Similarly, the expression levels of all three AMPK subunits were high at 4M (Fig. 1B), suggesting that AMPK might be transcriptionally activated by 20E signaling or starvation at ~4M to inhibit IIS.

Next, we tested the hypothesis that AMPK inhibits IIS in *Bombyx* both in vivo and in cultured cells. First, we treated L5D2 larvae with metformin, an AMPK activator that is a drug widely used to treat type 2 diabetes, or 5-aminoimidazole-4-carboxamide 1- β -D-ribofuranoside (AICAR), a cell permeable activator of AMPK. Notably, both metformin and AICAR not only promoted AMPK α phosphorylation but also inhibited the phosphorylation of InR and 4EBP in the fat body (Fig. 1C and D). Second, we treated 4M larvae with compound C, an ATP-competitive inhibitor of AMPK. In contrast, compound C inhibited AMPK α phosphorylation and simultaneously elevated the phosphorylation of InR and 4EBP in the fat body (Fig. 1E). These in vivo experiments strongly suggest that AMPK inhibits IIS in the *Bombyx* fat body. Third, we examined whether AMPK inhibits IIS in the *Bombyx* cell line DZNU-Bm-12 to the same extent as that in the *Bombyx* fat body. We treated DZNU-Bm-12 cells with AICAR, compound C, or both. The basal level of AMPK α phosphorylation was very low in the untreated DZNU-Bm-12 cells. The AICAR treatment dramatically activated AMPK in these cells, and this activation was markedly reduced following compound C treatment. In contrast, the untreated DZNU-Bm-12 cells showed high levels of InR phosphorylation and 4EBP phosphorylation. The AICAR treatment greatly reduced these phosphorylation levels both in the absence and presence of compound C (Fig. 1F). In addition to activating AMPK with chemicals, we overexpressed a constitutively active form of AMPK (V5-AMPK^{CA}) in DZNU-Bm-12 cells and found that the phosphorylation levels of both InR and 4EBP were inhibited by AMPK^{CA} (Fig. 1G). Thus, AMPK inhibits IIS in *Bombyx*.

AMPK Inhibits IIS in *Drosophila* Fat Body. To determine whether the inhibition of IIS by AMPK is conserved in other insects, we turned to *Drosophila*, the classic genetic and developmental model insect. First, we characterized the developmental profiles of phosphorylation levels of AMPK α at T172 (reflecting AMPK activity), InR at Y1135/1136 and AKT at S505 (reflecting IIS), and S6K at T398 and 4EBP at T37/46 (reflecting TORC1 activity) in the *Drosophila* fat body from the feeding stage of third-instar larvae to 6 h after puparium formation (6 h APF). The AMPK activity was low during the larval feeding stages, increased during the early wandering stage (EW), reached the maximal level during the late wandering stage (LW), remained high during the white prepupal stage (WPP), and decreased at 6 h APF (Fig. 2A). However, IIS and its downstream TORC1 activity exhibited profiles that were opposite to those of AMPK activity (Fig. 2A). Moreover, the protein level of AMPK α and

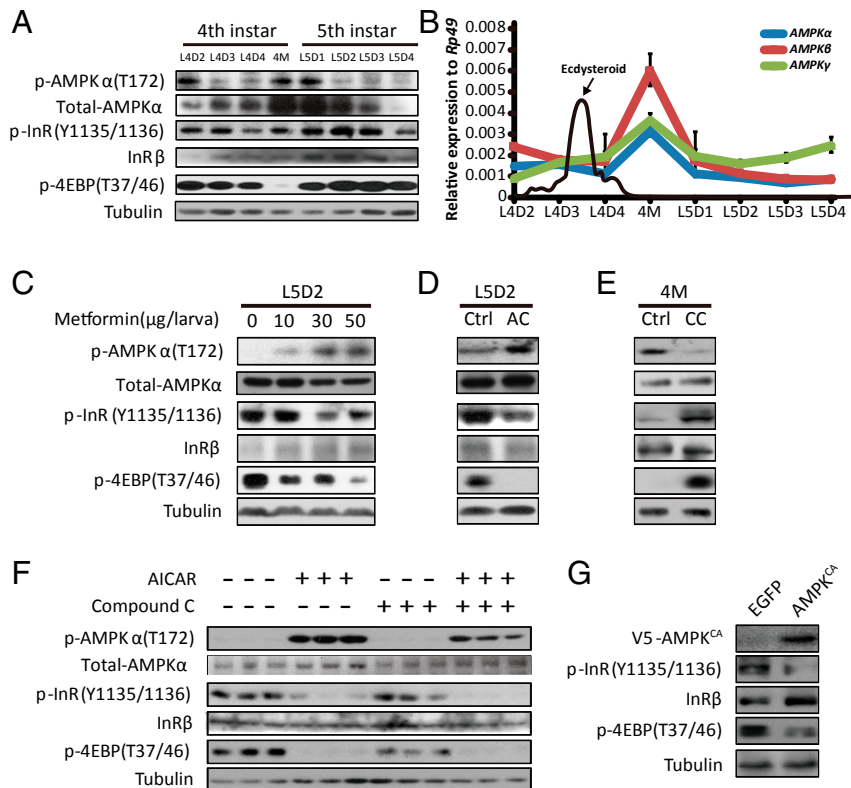


Fig. 1. AMPK inhibits IIS in *Bombyx*. (A) The developmental phosphorylation profile of AMPK, InR, and 4EBP in the *Bombyx* fat body from the early fourth instar to the prepupal stage. (B) The developmental profiles of mRNA levels of AMPK α (blue), AMPK β (red), and AMPK γ (green) in the *Bombyx* fat body as well as ecdysteroid titers (71) from the early fourth instar to the prepupal stage. Fold-changes shown are relative to *Rp49*. (C and D) Metformin or AICAR treatment activated AMPK and reduced the phosphorylation of InR and 4EBP. AC, the treatment of AICAR; Ctrl, control. (E) Compound C treatment reduced the phosphorylation of AMPK and promoted InR and 4EBP. CC, the treatment of compound C. (F) Phosphorylation levels of the target proteins when the *Bombyx* cell line DZNU-Bm-12 treated with AICAR, compound C, or both. (G) The phosphorylation levels of the target proteins when the active form of AMPK (V5-AMPK^{CA}) overexpressed constitutively in DZNU-Bm-12 cells. Note: Overexpression of EGFP was used as control.

the transcription levels of all three AMPK subunits exhibited developmental profiles that were quite similar to the profile of AMPK α phosphorylation from the larval feeding stage to WPP (Fig. 2 A and B), suggesting that 20E/starvation might transcriptionally activate AMPK to inhibit IIS during pupariation.

To confirm that AMPK indeed inhibits IIS in *Drosophila*, we genetically manipulated AMPK activity in the fat body of *Drosophila* larvae using the binary Gal4/UAS system. Driven by a fat body-specific Gal4 line (i.e., *Adh-Gal4*), a constitutively active form of AMPK (*UAS-AMPK^{CA}*) was overexpressed. The *AMPK^{CA}* overexpression greatly impeded IIS in the fat body during the larval feeding stages (Fig. 2C). To complement the gain-of-function studies, we employed another fat body-specific Gal4 line (i.e., *Lsp2-Gal4*) to overexpress a dominant-negative form of AMPK (*UAS-AMPK^{DN}*). In contrast, the *AMPK^{DN}* overexpression greatly increased IIS in the larval fat body at LW (Fig. 2D).

PI3K is an essential component of IIS. PI3K activity can be directly visualized in vivo using a reporter consisting of GFP fused to its pleckstrin homology domain tGPH. Thus, the tGPH membrane localization reflects PI3K activity and, thus, IIS (51). To clarify whether AMPK cell-autonomously regulates tGPH membrane localization and thus PI3K activity, we generated overexpression clones of *AMPK^{CA}* or *AMPK^{DN}* that were marked with RFP in the fat body using the *Drosophila* Flp-out technique. *AMPK^{CA}* overexpression inhibited tGPH membrane localization in the RFP⁺ clones when compared to the neighbor cells, supporting a cell-autonomous mechanism (Fig. 2E). In contrast, *AMPK^{DN}* overexpression cell-autonomously increased PI3K activity and, thus, IIS in mosaic clone cells (Fig. 2F). In conclusion,

AMPK inhibits IIS in the *Drosophila* fat body by reducing phosphorylation of at least two key components in IIS: InR and AKT.

AMPK Acts through PP2A to Inhibit IIS in *Drosophila* Fat Body. Since AMPK acts through PP2A to inactivate AKT in mammalian cells (45, 46, 52), we hypothesized that AMPK might also act through PP2A to antagonize IIS in the *Drosophila* fat body by dephosphorylating AKT, and probably InR. Importantly, the developmental profile of PP2A activity in the fat body underwent changes similar to that of AMPK activity from the feeding stage of third-instar larvae to 6 h APF (Fig. 3A). Moreover, PP2A activity in the larval fat body was significantly increased and decreased by *AMPK^{CA}* overexpression and *AMPK^{DN}* overexpression driven by *Lsp2-Gal4*, respectively (Fig. 3A), showing an AMPK-PP2A axis in the *Drosophila* fat body.

Then, we tested whether PP2A also inhibits IIS in the *Drosophila* fat body using both the Gal4/UAS system and Flp-out technique. Driven by *Lsp2-Gal4*, the overexpression of *PP2A^{CA}* and *PP2A^{DN}* greatly reduced and enhanced IIS in the larval fat body, respectively (Fig. 3B). Similarly, the overexpression of *PP2A^{CA}* and *PP2A^{DN}* cell-autonomously decreased and increased tGPH membrane localization and, thus, PI3K activity and IIS in larval fat body cells, respectively (Fig. 3C).

Since AMPK activates PP2A and both AMPK and PP2A inhibit IIS in the *Drosophila* fat body, we assumed that PP2A might mediate AMPK activity to inhibit IIS. To explore the inhibition of IIS by the AMPK-PP2A axis, we investigated the genetic interaction between AMPK and PP2A in the *Drosophila* fat

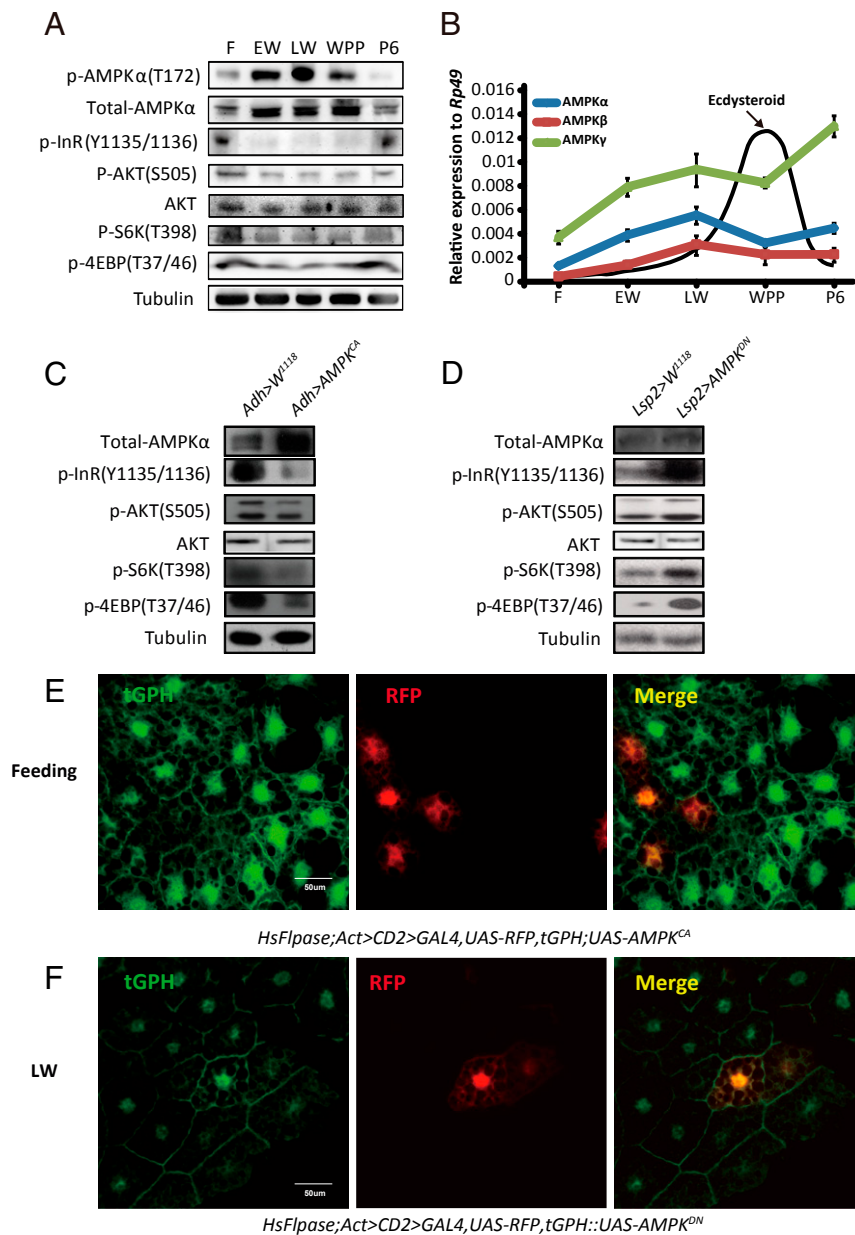


Fig. 2. AMPK inhibits IIS in *Drosophila*. (A) Developmental phosphorylation profile of AMPK, AKT, InR, S6K, and 4EBP in the *Drosophila* fat body at different stages (feeding, EW, LW, WPP, and 6 h after pupation). (B) Developmental profiles of mRNA levels of AMPK α (blue), AMPK β (red), and AMPK γ (green) in the *Drosophila* fat body and ecdysteroid titers (72, 73) at different stages. Fold-changes shown are relative to Rp49. (C) Phosphorylation levels of InR, AKT, S6K, and 4EBP were decreased in *Adh-Gal4 > UAS-AMPK^{CA}*. *Adh-Gal4* drives fat body-specific Gal4 expression. (D) Phosphorylation levels of InR, AKT, S6K, and 4EBP were increased in *Lsp2-Gal4 > UAS-AMPK^{DN}*. *Lsp2-Gal4* also drives fat body-specific Gal4 expression. (E) The Flp-out experiment revealing that the activity of PI3K is inhibited in red-positive clones in *HsFlpase; Act > CD2 > Gal4, UAS-RFP, tGPH; UAS-AMPK^{CA}* at the feeding stage. RFP (red), tGPH (green). (F) The Flp-out experiment revealing that the activity of PI3K is increased in red-positive clones in *HsFlpase; Act > CD2 > Gal4, UAS-RFP, tGPH::UAS-AMPK^{DN}* at the LW stage. RFP (red), tGPH (green).

body using both the Gal4/UAS system and Flp-out technique. Upon the simultaneous overexpression of *PP2A^{CA}* and *AMPK^{DN}*, *PP2A^{CA}* abolished the stimulatory effects of *AMPK^{DN}* on IIS. In contrast, upon the simultaneous overexpression of *PP2A^{DN}* and *AMPK^{CA}*, *PP2A^{DN}* continued to promote IIS even in the presence of *AMPK^{CA}* (Fig. 3 A and B). Furthermore, *PP2A* cell-autonomously mediated AMPK activity to inhibit tGPH membrane localization in the *Drosophila* fat body (Fig. 3C). According to these genetic interaction experiments in the *Drosophila* fat body, we conclude that AMPK acts through *PP2A* to inhibit IIS by dephosphorylating InR and AKT.

20E activates the AMPK-PP2A Axis and Inhibits IIS in Insect Fat Body. The 20E signaling plays a central role in triggering developmental transitions and, thus, limiting the growth period (7). As shown in Figs. 1–3, the activity of AMPK (and *PP2A* in *Drosophila*) was elevated, but IIS was reduced in the *Bombyx* fat body at ~4M and the *Drosophila* fat body during pupariation, suggesting that both the AMPK-PP2A axis and IIS in the fat body might be modulated by 20E or starvation to regulate the growth rate. To alter 20E signaling in *Bombyx*, we injected 20E on L5D2 and performed *USP* RNAi at the initiation of the wandering stage (19, 53). At 12 h after 20E treatment, the

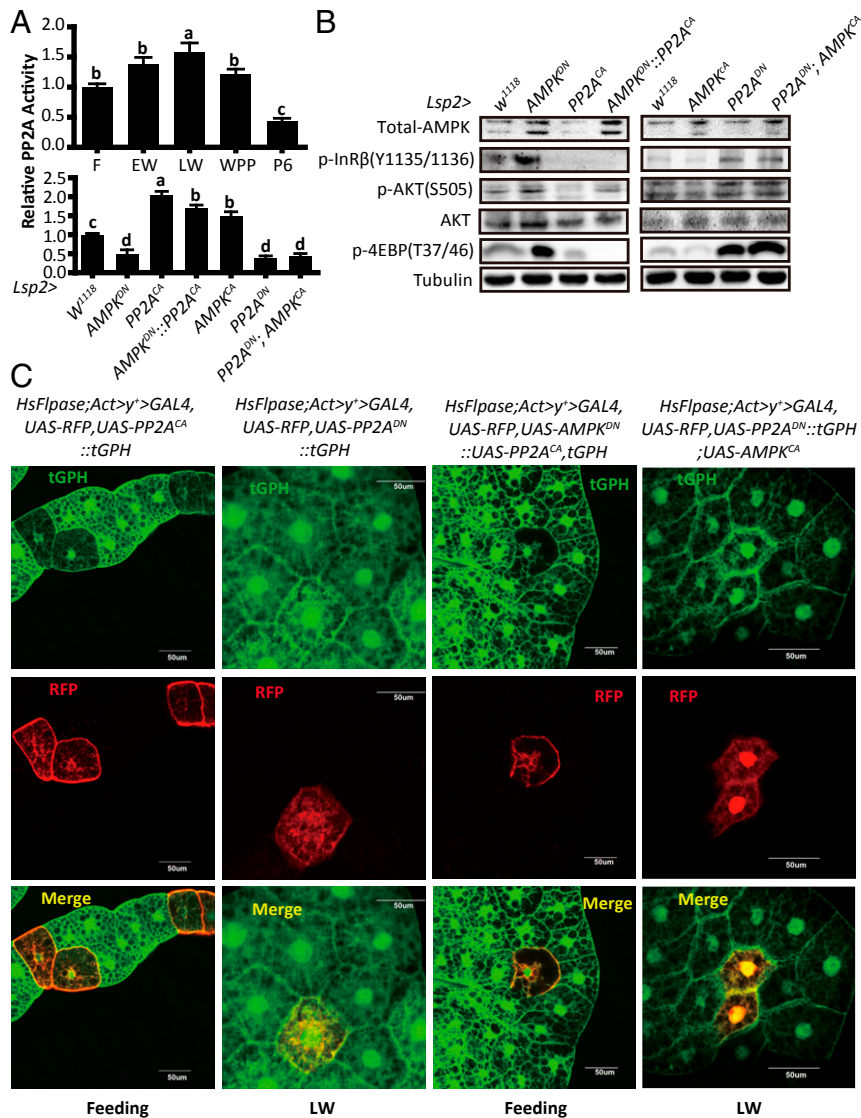


Fig. 3. AMPK acts through PP2A to inhibit IIS in *Drosophila* fat body. (A, Upper) Developmental profile of the relative PP2A activity in the *Drosophila* fat body at different stages (feeding, EW, LW, WPP, and 6 h after pupation). Fold-changes shown are relative to the feeding stage; (Lower) Relative PP2A activities in the fat body of different *Drosophila* genotypes (*W¹¹¹⁸*, *Lsp2-Gal4 > UAS-AMPK^{DN}*, *Lsp2-Gal4 > UAS-PP2A^{CA}*, *Lsp2-Gal4 > UAS-AMPK^{DN}::UAS-PP2A^{CA}*, *Lsp2-Gal4 > UAS-AMPK^{CA}*, *Lsp2-Gal4 > UAS-PP2A^{DN}*, and *Lsp2-Gal4 > UAS-PP2A^{DN}; UAS-AMPK^{CA}*). Fold-changes shown are relative to the *W¹¹¹⁸*. Statistical significance between samples was evaluated using ANOVA: Bars labeled with different lowercase letters are significantly different ($P < 0.05$). (B) Western blot analysis results in the fat body of different *Drosophila* genotypes as in A, Lower. (C) A Flip-out experiment revealing that the activity of PI3K is decreased in red-positive clones in *HsFlpase; Act > y⁺ > Gal4, UAS-RFP, tGPH::UAS-PP2A^{CA}* and *HsFlpase; Act > y⁺ > Gal4, UAS-RFP, UAS-AMPK^{DN}::UAS-PP2A^{CA}, tGPH* at the feeding stage, while the activity of PI3K is increased in *HsFlpase; Act > y⁺ > Gal4, UAS-RFP, UAS-PP2A^{DN}*, and *HsFlpase; Act > y⁺ > Gal4, UAS-RFP, UAS-PP2A^{DN}::tGPH; UAS-AMPK^{CA}* at the LW stage. RFP (red), tGPH (green).

AMPK activity in the fat body greatly increased, whereas IIS vastly decreased. In contrast, 24 h after the *USP* RNAi treatment, the AMPK activity in the fat body decreased, whereas IIS increased (Fig. 4A). To manipulate 20E signaling in *Drosophila*, we added 20E to the diet during the feeding stages of the third larval instar and overexpressed a dominant-negative form of *Ecr* (*UAS-Ecr^{DN}*) in the larval fat body using both the Gal4/UAS system and Flip-out technique. At 12 h after 20E treatment, the activity of AMPK and PP2A in the fat body increased, whereas IIS decreased. In contrast, *Ecr^{DN}* overexpression decreased the activity of AMPK and PP2A and increased IIS in the larval fat body at LW (Fig. 4B–E). Altogether, 20E activates the AMPK-PP2A axis and inhibits IIS in the insect fat body.

Since the protein level of AMPK α and the mRNA levels of all three AMPK subunits in the fat body exhibits developmental

profiles that are similar to the activity profile of AMPK in *Bombyx* or the activity profiles of AMPK and PP2A in *Drosophila* (Figs. 1–3), we investigated the possibility that 20E might transcriptionally activate AMPK to promote PP2A activity and inhibit IIS. In *Bombyx*, the 20E treatment induced the expression of AMPK α , AMPK β , and AMPK γ in the fat body, while *USP* RNAi decreased their expression (Fig. 4F and G). Similarly, in *Drosophila* 20E treatment and *Ecr^{DN}* overexpression up-regulated and down-regulated the mRNA levels of all three AMPK subunits, respectively (Fig. 4H and I). Altogether, our hypothesis that AMPK is transcriptionally activated by 20E to inhibit IIS in the insect fat body is supported.

Because both *Bombyx* and *Drosophila* larvae cease feeding at ~4M and during pupariation, respectively, AMPK activity is also likely regulated by the poor nutrition status coordinated by 20E

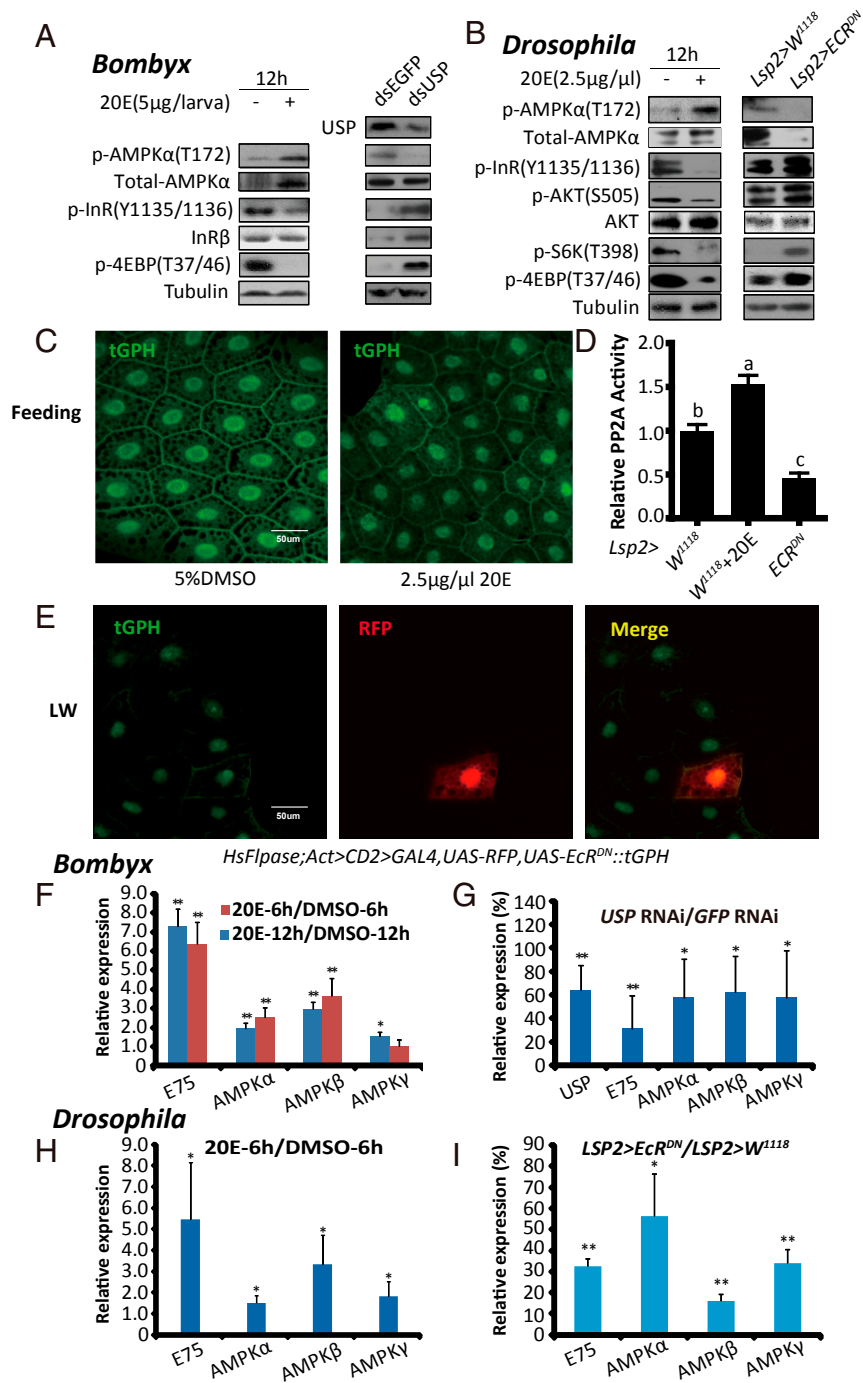


Fig. 4. 20E activates the AMPK-PP2A axis and inhibits IIS in insect fat body. (A) p-AMPK α , total-AMPK α , p-InR, and p-4EBP levels were measured after the 20E treatment (5 μ g per larva) or USP RNAi in *Bombyx*. (A, Right) Anti-USP was used. (B) The levels of p-AMPK α , total-AMPK α , p-InR, p-AKT, p-S6K, and p-4EBP were measured in 20E-fed (2.5 μ g/ μ L) or *Lsp2* > *Ecr^{DN}* *Drosophila*. (C) tGPH membrane localization in the fat body of *Drosophila* following different treatments (5% DMSO and 2.5 μ g/ μ L 20E). tGPH (green). (D) Relative PP2A activity in 20E-fed (2.5 μ g/ μ L) or *Lsp2* > *Ecr^{DN}* *Drosophila*. Fold-changes shown are relative to the *W¹¹¹⁸*. Statistical significance between samples was evaluated using ANOVA: Bars labeled with different lowercase letters are significantly different ($P < 0.05$). (E) Flp-out experiment revealing that the activity of PI3K is increased in red-positive clones in *HsFlpase; Act > CD2 > Gal4, UAS-RFP, UAS-Ecr^{DN}::tGPH* at the LW stage. RFP (red), tGPH (green). (F and G) mRNA levels of AMPK α , AMPK β , and AMPK γ in the fat body of *Bombyx* following 20E treatment (6 h and 12 h) or USP RNAi. Fold-changes shown are relative to DMSO treatment or GFP RNAi, respectively. (H and I) mRNA levels of AMPK α , AMPK β , and AMPK γ in the fat body of *Drosophila* 6 h after the 20E treatment or *Lsp2* > *Ecr^{DN}*. Fold-changes shown are relative to DMSO treatment or *Lsp2* > *W¹¹¹⁸*, respectively. Statistical significance between samples was evaluated using Student's *t* test (** $P < 0.05$, *** $P < 0.01$).

signaling (8, 9, 25, 26). Then, we extended our investigation to the mechanism by which 20E-induced starvation-like conditions activate AMPK in the *Bombyx* fat body (54–56). At 12 h, but not 6 h, after L5D2 larvae were injected with 20E, AMPK was

activated in the fat body, and the activation increased at 24 h after the 20E injection (Fig. 4A and *SI Appendix, Fig. S24*), suggesting that 20E slowly elevated AMPK activity. In contrast to the slow activation of AMPK by 20E, starvation activated

AMPK in the fat body within 6 h, and the rapid activation of AMPK by starvation was attenuated by refeeding the starved larvae with mulberry leaves for 3 h or a longer period after a 12-h starvation pretreatment (SI Appendix, Fig. S2 B and C). To further corroborate that the AMPK activity in the fat body depends on the energy status, we injected glucose or leucine into starved larvae or larvae at 4M and examined the changes in AMPK activity and IIS. Importantly, glucose inhibited AMPK activity and induced IIS and 4EBP phosphorylation. However, leucine had no effects on AMPK activity or InR phosphorylation but greatly induced 4EBP phosphorylation (SI Appendix, Fig. S2D). Therefore, in addition to the transcriptional activation of AMPK, 20E should also slowly induce a sugar starvation-like condition to activate AMPK (54–56).

The AMPK-PP2A Axis Is Required for 20E to Antagonize IIS in Insect Fat Body. The results mentioned above showed that 20E activates the AMPK-PP2A axis and inhibits IIS in the insect fat body (Figs. 1–4). Next, we examined whether the AMPK-PP2A axis is required for 20E to antagonize IIS in both *Bombyx* and *Drosophila*. As shown in Fig. 1E, compound C inhibited AMPK activity in the *Bombyx* fat body and elevated IIS at ~4M when 20E signaling is high, while injection of 20E into L5D2 larvae increased the AMPK activity and blocked IIS in the fat body. Importantly, a simultaneous injection of the AMPK inhibitor compound C nearly abolished the stimulatory effects of 20E on AMPK activity and its inhibitory effects on IIS (Fig. 5A). According to the results presented in Figs. 2 D and F and 3 B and C, *AMPK^{DN}* overexpression inhibited PP2A activity in the *Drosophila* fat body and elevated IIS at LW when 20E signaling is high. Using the Flp-out technique, *AMPK^{DN}* overexpression interdicted the inhibitory effects of 20E on PI3K activity and, thus, IIS in mosaic clone cells (Fig. 5B). Similar to *AMPK^{DN}* overexpression, *PP2A^{DN}* overexpression cell-autonomously blocked the inhibition by 20E (Fig. 5C). Altogether, the AMPK-PP2A axis is activated by and required for 20E to antagonize IIS in the insect fat body.

Activation of the AMPK-PP2A Axis and Inhibition of IIS in Insect Fat Body Reduce Food Consumption and Restrict Growth Rate. After demonstrating that the AMPK-PP2A axis is activated by 20E to antagonize IIS in the insect fat body, we examined the possible role of AMPK-PP2A activation by 20E in controlling the larval growth rate. We injected *Bombyx* larvae with the AMPK activators metformin and AICAR on L5D2. Metformin and AICAR dose-dependently resulted in larval lethality, a reduction in the larval growth rate, a decrease in larval body weight, a delay in pupation, and a decrease in food consumption (Fig. 6 A–D and SI Appendix, Figs. S3 and S4). We previously found that the PI3K inhibitor wortmannin exerted inhibitory effects on larval growth, development, and feeding (57). Thus, the AMPK activators and PI3K inhibitor similarly inhibited growth, development, and feeding in *Bombyx* larvae.

Finally, we examined whether the specific activation of the AMPK-PP2A axis in the *Drosophila* larval fat body is sufficient to reduce the growth rate as shown by the inhibition of IIS in the *Drosophila* larval fat body (9, 58, 59). Similar to the fat body-specific overexpression of *P TEN* and *Dp110^{DN}* to suppress IIS, the fat body-specific overexpression of *AMPK^{CA}* and *PP2A^{CA}* to activate the AMPK-PP2A axis resulted in a reduction of larval growth rate, a delay in pupation, and decreases in pupa size, body weight, and food consumption; significant lethality was also observed following *PP2A^{CA}* overexpression (Fig. 6 E–H and SI Appendix, Fig. S5 A and B). In addition, fat body-specific overexpression of *AMPK^{DN}*, *PP2A^{DN}*, and *Dp110^{CA}* generally increased developmental timing and body weight. Since these animals grew bigger with delayed developmental timing, their larvae might consume more food than the control animals (SI Appendix, Fig. S5 C and D).

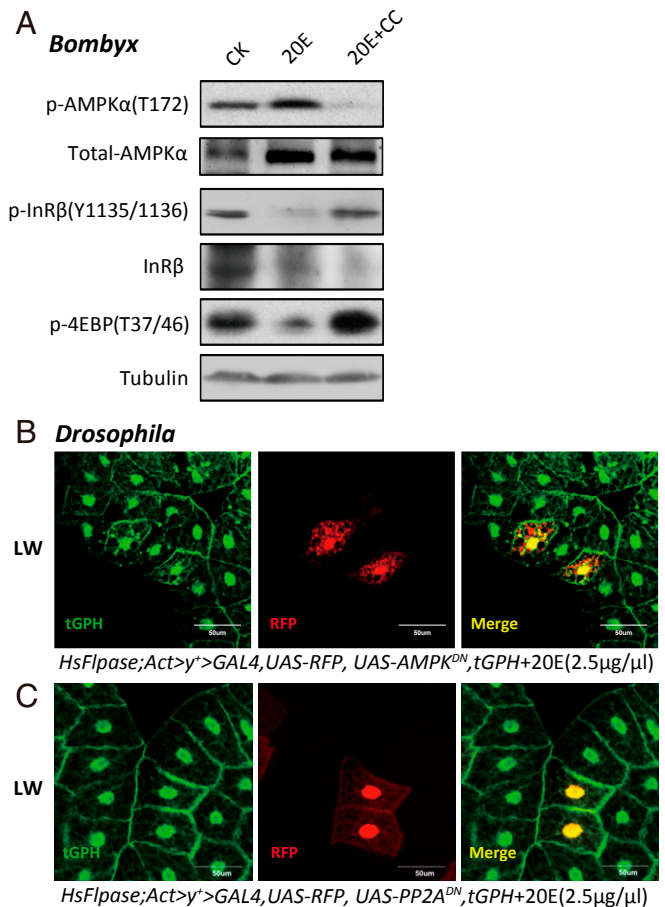


Fig. 5. The AMPK-PP2A axis is required for 20E to antagonize IIS in insect fat body. (A) p-AMPK α , total-AMPK α , p-InR, and p-4EBP levels were measured in *Bombyx* following treatment with 20E and compound C. CC, compound C; CK, control. (B and C) Flp-out experiment revealing that the activity of PI3K is increased in red-positive clones in *HsFlpase; Act > y+ > Gal4, UAS-RFP, tGPH::UAS-AMPK^{DN}* (B) or *HsFlpase; Act > y+ > Gal4, UAS-RFP, tGPH::UAS-PP2A^{DN}* (C) following 20E treatment (2.5 $\mu\text{g}/\mu\text{l}$) at the LW stage. RFP (red), tGPH (green).

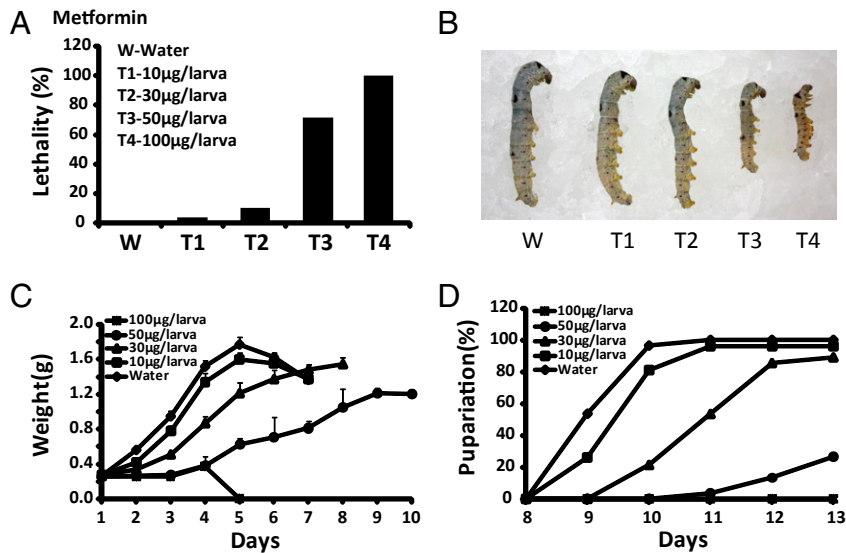
In summary, the AMPK-PP2A axis in insect fat body is activated by 20E to antagonize IIS and reduce food consumption, resulting in the restriction of growth rate and body weight. (SI Appendix, Fig. S6).

Discussion

Activation of AMPK Is Induced by 20E Signaling in Two Ways. In this study, we discovered that in the insect fat body, 20E activates AMPK in two ways: By up-regulating the mRNA levels of all three AMPK subunits and by inducing energy stress to activate AMPK (SI Appendix, Fig. S6).

The transcription levels of all three AMPK subunits, the protein level of AMPK α , and the phosphorylation level of AMPK α were all elevated in the *Bombyx* fat body at ~4M and in the *Drosophila* fat body during pupariation, showing developmental profiles that were consistent with those of 20E signaling (Figs. 1 and 2). Both the gain-of-function and loss-of-function experiments further demonstrate that AMPK is transcriptionally activated by 20E signaling (Fig. 4). According to our preliminary data, 20E-EcR-USP does not directly induce the expression of the AMPK-PP2A subunit genes, and further studies should be performed to investigate the detailed

Bombyx



Drosophila

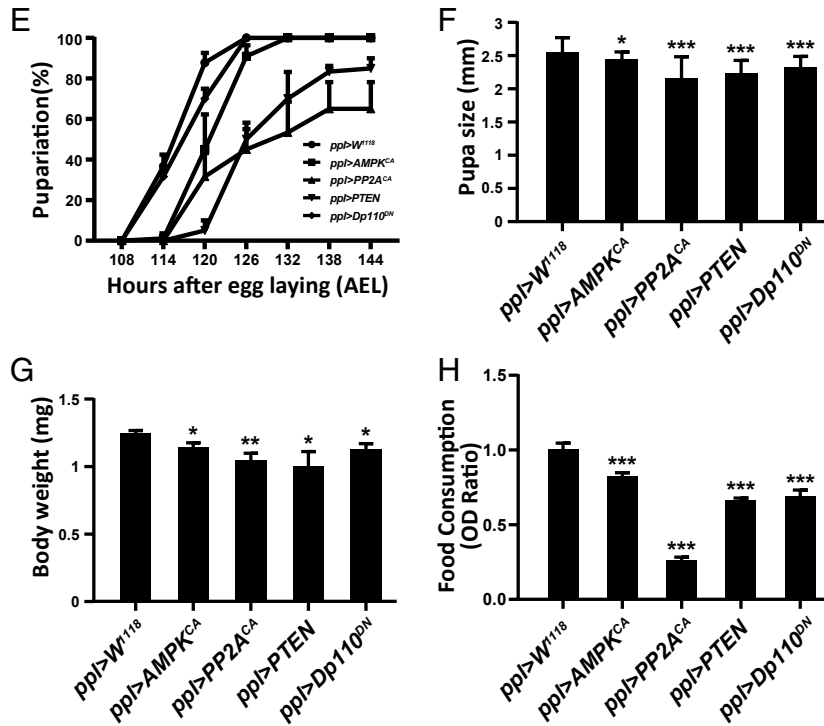


Fig. 6. Activation of AMPK-PP2A axis and inhibition of IIS in insect fat body reduce food consumption and restrict growth rate. (A–D) Changes in lethality (A), phenotype (B), body weight (C), and percentage of pupariation (D) following the metformin treatment of different dosages in *Bombyx* on L5D2. (E–H) Changes in percentage of pupariation (E), pupa size (F), body weight (G), and food consumption (H) in *ppl > W¹¹¹⁸* (control), *ppl > AMPK^{CA}*, *ppl > PP2A^{CA}*, *ppl > PTEN*, and *ppl > Dp110^{DN}*. **P* < 0.05, ***P* < 0.01, ****P* < 0.001.

mechanisms whereby the 20E-triggered transcriptional cascade is involved in this transcriptional activation.

20E is well known to act through the insect larval central nervous system (CNS) to induce wandering behavior and escape from food (60, 61). Moreover, 20E slowly reduces insect feeding behavior and, thus, food consumption (54, 55). Nevertheless, both the induction of wandering behavior and the reduction of feeding behavior can cause energy stress, such as sugar starvation, which ultimately increases the cellular AMP/ATP ratio, leading to the activation of AMPK (31–34). According to the

Bombyx fat body results at ~4M, such a poor nutrition status promoted AMPK activity and inhibited IIS (SI Appendix, Fig. S2). Altogether, 20E slowly induces a sugar starvation-like condition to activate AMPK in the fat body by modulating CNS-controlled feeding behavior and wandering behavior in insects.

Roles of the AMPK-PP2A Axis Are Linked to the Antagonism of IIS by 20E. As summarized in the Introduction, IIS is an anabolic pathway, while AMPK accounts for catabolism, thus it naturally exists a mutual inhibition between IIS and AMPK. AMPK and

PP2A might affect each other, and the AMPK-PP2A axis has been documented in mammalian cells (45, 46). In this study, we confirmed that the AMPK-PP2A axis exists in the *Drosophila* fat body (Fig. 3), linking the antagonism of IIS by 20E (Figs. 3–5).

In addition to the dephosphorylation of AKT by PP2A (45), PP2A also dephosphorylates S6K (62), playing a key role in the attenuation of IIS and its downstream TORC1 activity. Our studies determined that PP2A not only dephosphorylates AKT and inhibits TORC1 activity but also dephosphorylates InR and inactivates PI3K, showing that PP2A inhibits IIS starting from the dephosphorylation of InR (Fig. 3). We hypothesize that PP2A might dephosphorylate InR, PI3K, and AKT and, thus, inhibit IIS in an integrative manner.

Finally, we demonstrated that 20E activates the AMPK-PP2A axis to antagonize IIS in the insect fat body (Fig. 4). After blocking either AMPK or PP2A, 20E no longer antagonizes IIS in the fat body (Fig. 5). In summary, the AMPK-PP2A axis in the insect fat body is activated by 20E to antagonize IIS.

Considering the similar regulatory functions in the antagonism of IIS by 20E, we examined the possible relationship between miR-8/Ush (11, 27) and AMPK-PP2A. Via bioinformatics prediction, we found that miR-8 does not target AMPK or PP2A transcripts. Meanwhile, our preliminary data showed that overexpression of *AMPK^{CA}* or *PP2A^{CA}* did not affect *Ush* expression in the fat body. Thus, we suppose that AMPK-PP2A should function in parallel with miR-8 in the antagonism of IIS by 20E. We conclude that the AMPK-PP2A axis is a crucial, but not a unique, pathway linking 20E to IIS.

Activation of the AMPK-PP2A Axis and Inhibition of IIS in Insect Fat Body Restrict Larval Growth Rate. The previous studies (9, 58, 59) and our results (Fig. 6 and *SI Appendix*, Fig. S5) together indicate that, similar to the inhibition of IIS in the larval fat body, activation of the fat body AMPK-PP2A axis reduces food consumption and thus restricts growth rate and body size in *Drosophila* (*SI Appendix*, Fig. S6). In other words, the AMPK-PP2A axis and IIS in the fat body play opposite developmental roles in regulating the larval growth rate and body size, and one crucial reason should be the modulation of feeding behavior and thus food consumption.

The insect fat body, which is analogous to the mammalian liver, functions as an energy reservoir and nutrient sensor to regulate developmental timing (12, 13, 63). Fat body-derived amino acid signals, which involve Slimfast (the amino acid transporter) and TORC1 signaling, reactivate quiescent neuroblasts and finally control larval growth by regulating the synthesis and release of insulin/IGF (64–66). In addition to amino acid-dependent signals, certain other growth-promoting factors, such

as CCHamide-2 and Unpaired 2, secreted from the fat body also affect the brain to remotely control insulin/IGF secretion in *Drosophila* (67, 68). Moreover, IIS acts as the center of energy and nutrition response and positively regulates the larval growth rate partially by inhibiting autophagy in the *Drosophila* fat body (8, 16, 69, 70). In contrast, 20E negatively regulates the larval growth rate by impeding IIS in the *Drosophila* fat body (9). Interestingly, our preliminary results suggest that the AMPK-PP2A axis had little effect on fat body autophagy during normal feeding conditions and that TORC1 in the fat body plays little role in regulating the larval growth rate.

It is likely that activation of the AMPK-PP2A axis and the inhibition of IIS in the fat body might affect the nutritional and endocrinal functions of this tissue. These changes in the fat body should cause the reduction of food consumption, resulting in the restriction of growth rate and body size. Investigating the detailed molecular mechanisms of how food consumption and its related feeding behavior and wandering behavior are regulated by hormonal and nutritional signals in the fat body might open a new window for understanding the regulatory mechanisms of final body size in insects. In future, it is worthwhile to examine whether the CNS, as well as neuropeptides and neurotransmitters, are involved in this regulation. Taking these data together, we propose a model in which 20E antagonizes IIS by activating the AMPK-PP2A axis in the fat body to restrict the larval growth rate in insects (*SI Appendix*, Fig. S6). This study expands our understanding of the comprehensive regulatory mechanisms underlying final body size determination in animals.

Data Availability. All data are available within this report and the associated *SI Appendix*.

Materials and Methods

A detailed description of the materials and methods used in this study is provided in *SI Appendix*, *SI Materials and Methods*. *Bombyx*, a number of fly strains, and *Drosophila* genetics were used. Western blot analysis, dsRNA injection, PP2A activity assay, food intake assay, and imaging were performed. Developmental timing was analyzed by recording pupariation. Chemicals, cell culture, and qPCR were described. See *SI Appendix*, Table S1 for a list of all primers used.

ACKNOWLEDGMENTS. We thank P. Leopold and T. P. Neufeld for their great comments and suggestions to improve this paper; and J. Chung, B. A. Edgar, P. Chervas, and the Bloomington *Drosophila* Stock Center for fly stocks. This study was supported by the National Science Foundation of China Grants 31620103917, 31330072, and 31702054, and the National Key Research and Development Program of China Grant 2016YFD0101900 (to S. Li and S. Liu); and the Natural Science Foundation of Chongqing Municipal Education Commission Grant KJ1400410 (to Y.X.).

1. I. Conlon, M. Raff, Size control in animal development. *Cell* **96**, 235–244 (1999).
2. R. H. Gokhale, A. W. Shingleton, Size control: The developmental physiology of body and organ size regulation. *Wiley Interdiscip. Rev. Dev. Biol.* **4**, 335–356 (2015).
3. H. F. Nijhout, The control of body size in insects. *Dev. Biol.* **261**, 1–9 (2003).
4. H. F. Nijhout, V. Callier, Developmental mechanisms of body size and wing-body scaling in insects. *Annu. Rev. Entomol.* **60**, 141–156 (2015).
5. H. F. Nijhout *et al.*, The developmental control of size in insects. *Wiley Interdiscip. Rev. Dev. Biol.* **3**, 113–134 (2014).
6. D. R. Nässel, J. Vanden Broeck, Insulin/IGF signaling in *Drosophila* and other insects: Factors that regulate production, release and post-release action of the insulin-like peptides. *Cell. Mol. Life Sci.* **73**, 271–290 (2016).
7. N. Yamanaka, K. F. Rewitz, M. B. O'Connor, Ecdysone control of developmental transitions: Lessons from *Drosophila* research. *Annu. Rev. Entomol.* **58**, 497–516 (2013).
8. T. E. Rusten *et al.*, Programmed autophagy in the *Drosophila* fat body is induced by ecdysone through regulation of the PI3K pathway. *Dev. Cell* **7**, 179–192 (2004).
9. J. Colombani *et al.*, Antagonistic actions of ecdysone and insulins determine final size in *Drosophila*. *Science* **310**, 667–670 (2005).
10. B. Keshan, B. Thounaojam, S. D. Kh, Insulin and 20-hydroxyecdysone action in *Bombyx mori*: Glycogen content and expression pattern of insulin and ecdysone receptors in fat body. *Gen. Comp. Endocrinol.* **241**, 108–117 (2017).
11. H. Jin, V. N. Kim, S. Hyun, Conserved microRNA miR-8 controls body size in response to steroid signaling in *Drosophila*. *Genes Dev.* **26**, 1427–1432 (2012).
12. E. L. Arrese, J. L. Soulages, Insect fat body: Energy, metabolism, and regulation. *Annu. Rev. Entomol.* **55**, 207–225 (2010).
13. L. Boulan, M. Milán, P. Léopold, The systemic control of growth. *Cold Spring Harb. Perspect. Biol.* **7**, a019117 (2015).
14. S. Li, X. Yu, Q. Feng, Fat body biology in the last decade. *Annu. Rev. Entomol.* **64**, 315–333 (2019).
15. T. P. Neufeld, Autophagy and cell growth—The yin and yang of nutrient responses. *J. Cell Sci.* **125**, 2359–2368 (2012).
16. R. C. Scott, O. Schuldiner, T. P. Neufeld, Role and regulation of starvation-induced autophagy in the *Drosophila* fat body. *Dev. Cell* **7**, 167–178 (2004).
17. H. Liu, Q. Jia, G. Tettamanti, S. Li, Balancing crosstalk between 20-hydroxyecdysone-induced autophagy and caspase activity in the fat body during *Drosophila* larval-prepupal transition. *Insect Biochem. Mol. Biol.* **43**, 1068–1078 (2013).
18. H. Liu, J. Wang, S. Li, E93 predominantly transduces 20-hydroxyecdysone signaling to induce autophagy and caspase activity in *Drosophila* fat body. *Insect Biochem. Mol. Biol.* **45**, 30–39 (2014).
19. L. Tian *et al.*, 20-Hydroxyecdysone upregulates Atg genes to induce autophagy in the *Bombyx* fat body. *Autophagy* **9**, 1172–1187 (2013).
20. C. K. Mirth, A. W. Shingleton, The roles of juvenile hormone, insulin/target of rapamycin, and ecdysone signaling in regulating body size in *Drosophila*. *Commun. Integr. Biol.* **7**, e971568 (2014).
21. Y. Wei *et al.*, TORC1 regulators Iml1/GATOR1 and GATOR2 control meiotic entry and oocyte development in *Drosophila*. *Proc. Natl. Acad. Sci. U.S.A.* **111**, E5670–E5677 (2014).
22. I. Ruvinsky, O. Meyuhas, Ribosomal protein S6 phosphorylation: From protein synthesis to cell size. *Trends Biochem. Sci.* **31**, 342–348 (2006).

23. A. Barthel, D. Schmoll, T. G. Unterman, FoxO proteins in insulin action and metabolism. *Trends Endocrinol. Metab.* **16**, 183–189 (2005).
24. B. Gershman *et al.*, High-resolution dynamics of the transcriptional response to nutrition in *Drosophila*: A key role for dFOXO. *Physiol. Genomics* **29**, 24–34 (2007).
25. M. S. Hossain *et al.*, 20-Hydroxyecdysone-induced transcriptional activity of FoxO upregulates brummer and acid lipase-1 and promotes lipolysis in *Bombyx* fat body. *Insect Biochem. Mol. Biol.* **43**, 829–838 (2013).
26. M. J. Cai *et al.*, 20-Hydroxyecdysone activates Forkhead box O to promote proteolysis during *Helicoverpa armigera* molting. *Development* **143**, 1005–1015 (2016).
27. S. Hyun *et al.*, Conserved MicroRNA miR-8/miR-200 and its target USH/FOG2 control growth by regulating PI3K. *Cell* **139**, 1096–1108 (2009).
28. K. Buhler *et al.*, Growth control through regulation of insulin signalling by nutrition-activated steroid hormone in *Drosophila*. *Development* **145**, dev165654 (2018).
29. D. G. Hardie, AMP-activated/SNF1 protein kinases: Conserved guardians of cellular energy. *Nat. Rev. Mol. Cell Biol.* **8**, 774–785 (2007).
30. D. G. Hardie, F. A. Ross, S. A. Hawley, AMPK: A nutrient and energy sensor that maintains energy homeostasis. *Nat. Rev. Mol. Cell Biol.* **13**, 251–262 (2012).
31. L. Shang *et al.*, Nutrient starvation elicits an acute autophagic response mediated by Ulk1 dephosphorylation and its subsequent dissociation from AMPK. *Proc. Natl. Acad. Sci. U.S.A.* **108**, 4788–4793 (2011).
32. D. G. Hardie, AMPK—Sensing energy while talking to other signaling pathways. *Cell Metab.* **20**, 939–952 (2014).
33. D. G. Hardie, AMPK: Positive and negative regulation, and its role in whole-body energy homeostasis. *Curr. Opin. Cell Biol.* **33**, 1–7 (2015).
34. S. K. Hindupur, A. González, M. N. Hall, The opposing actions of target of rapamycin and AMP-activated protein kinase in cell growth control. *Cold Spring Harb. Perspect. Biol.* **7**, a019141 (2015).
35. J. H. Lee *et al.*, Energy-dependent regulation of cell structure by AMP-activated protein kinase. *Nature* **447**, 1017–1020 (2007).
36. M. Lippai *et al.*, SNF4Agamma, the *Drosophila* AMPK gamma subunit is required for regulation of developmental and stress-induced autophagy. *Autophagy* **4**, 476–486 (2008).
37. R. A. Miller, M. J. Birnbaum, An energetic tale of AMPK-independent effects of metformin. *J. Clin. Invest.* **120**, 2267–2270 (2010).
38. J. I. Partanen, A. I. Nieminen, T. P. Mäkelä, J. Klefstrom, Suppression of oncogenic properties of c-Myc by LKB1-controlled epithelial organization. *Proc. Natl. Acad. Sci. U.S.A.* **104**, 14694–14699 (2007).
39. M. Funakoshi *et al.*, A gain-of-function screen identifies wdb and lkb1 as lifespan-extending genes in *Drosophila*. *Biochem. Biophys. Res. Commun.* **405**, 667–672 (2011).
40. J. Kim, M. Kundu, B. Viollet, K. L. Guan, AMPK and mTOR regulate autophagy through direct phosphorylation of Ulk1. *Nat. Cell Biol.* **13**, 132–141 (2011).
41. D. M. Gwinn *et al.*, AMPK phosphorylation of raptor mediates a metabolic checkpoint. *Mol. Cell* **30**, 214–226 (2008).
42. A. Hahn-Windgassen *et al.*, Akt activates the mammalian target of rapamycin by regulating cellular ATP level and AMPK activity. *J. Biol. Chem.* **280**, 32081–32089 (2005).
43. S. Horman *et al.*, Insulin antagonizes ischemia-induced Thr172 phosphorylation of AMP-activated protein kinase alpha-subunits in heart via hierarchical phosphorylation of Ser485/491. *J. Biol. Chem.* **281**, 5335–5340 (2006).
44. S. Kovacic *et al.*, Akt activity negatively regulates phosphorylation of AMP-activated protein kinase in the heart. *J. Biol. Chem.* **278**, 39422–39427 (2003).
45. K. Y. Kim *et al.*, Adiponectin-activated AMPK stimulates dephosphorylation of AKT through protein phosphatase 2A activation. *Cancer Res.* **69**, 4018–4026 (2009).
46. S. Park, T. L. Scheffler, S. S. Rossie, D. E. Gerrard, AMPK activity is regulated by calcium-mediated protein phosphatase 2A activity. *Cell Calcium* **53**, 217–223 (2013).
47. S. Zheng, Z. Qu, M. Zanetti, B. Lam, I. Chin-Sang, C. elegans PTEN and AMPK block neuroblast divisions by inhibiting a BMP-insulin-PP2A-MAPK pathway. *Development* **145**, dev166876 (2018).
48. B. K. Joseph *et al.*, Inhibition of AMP kinase by the protein phosphatase 2A heterotrimer, PP2A^{Ppp2r2d}. *J. Biol. Chem.* **290**, 10588–10598 (2015).
49. S. Padmanabhan *et al.*, A PP2A regulatory subunit regulates *C. elegans* insulin/IGF-1 signaling by modulating AKT-1 phosphorylation. *Cell* **136**, 939–951 (2009).
50. Y. Wu, P. Song, J. Xu, M. Zhang, M. H. Zou, Activation of protein phosphatase 2A by palmitate inhibits AMP-activated protein kinase. *J. Biol. Chem.* **282**, 9777–9788 (2007).
51. J. S. Britton, W. K. Lockwood, L. Li, S. M. Cohen, B. A. Edgar, *Drosophila*'s insulin/PI3-kinase pathway coordinates cellular metabolism with nutritional conditions. *Dev. Cell* **2**, 239–249 (2002).
52. Y.-C. Kuo *et al.*, Regulation of phosphorylation of Thr-308 of Akt, cell proliferation, and survival by the B55 α regulatory subunit targeting of the protein phosphatase 2A holoenzyme to Akt. *J. Biol. Chem.* **283**, 1882–1892 (2008).
53. L. Tian *et al.*, Genome-wide regulation of innate immunity by juvenile hormone and 20-hydroxyecdysone in the *Bombyx* fat body. *BMC Genomics* **11**, 549 (2010).
54. Y. Tanaka, K. Asaoka, S. Takeda, Different feeding and gustatory responses to ecdysone and 20-hydroxyecdysone by larvae of the silkworm, *Bombyx mori*. *J. Chem. Ecol.* **20**, 125–133 (1994).
55. S. Wang *et al.*, 20-hydroxyecdysone reduces insect food consumption resulting in fat body lipolysis during molting and pupation. *J. Mol. Cell Biol.* **2**, 128–138 (2010).
56. Y. Li *et al.*, Integrative proteomics and metabolomics analysis of insect larva brain: Novel insights into the molecular mechanism of insect wandering behavior. *J. Proteome Res.* **15**, 193–204 (2016).
57. L. Ma *et al.*, Ras1(CA) overexpression in the posterior silk gland improves silk yield. *Cell Res.* **21**, 934–943 (2011).
58. R. Delanoue, M. Slaidina, P. Léopold, The steroid hormone ecdysone controls systemic growth by repressing dMyc function in *Drosophila* fat cells. *Dev. Cell* **18**, 1012–1021 (2010).
59. V. A. Francis, A. Zorzano, A. A. Teleman, dDOR is an EcR coactivator that forms a feed-forward loop connecting insulin and ecdysone signaling. *Curr. Biol.* **20**, 1799–1808 (2010).
60. O. S. Dominick, J. W. Truman, The physiology of wandering behaviour in *Manduca sexta*. IV. Hormonal induction of wandering behaviour from the isolated nervous system. *J. Exp. Biol.* **121**, 133–151 (1986).
61. O. S. Dominick, J. W. Truman, The physiology of wandering behaviour in *Manduca sexta*. III. Organization of wandering behaviour in the larval nervous system. *J. Exp. Biol.* **121**, 115–132 (1986).
62. R. T. Peterson, B. N. Desai, J. S. Hardwick, S. L. Schreiber, Protein phosphatase 2A interacts with the 70-kDa S6 kinase and is activated by inhibition of FKBP12-rapamycin-associated protein. *Proc. Natl. Acad. Sci. U.S.A.* **96**, 4438–4442 (1999).
63. Y. Zhang, Y. Xi, Fat body development and its function in energy storage and nutrient sensing in *Drosophila melanogaster*. *J. Tissue Sci. Eng.* **6**, 141 (2015).
64. J. Colombani *et al.*, A nutrient sensor mechanism controls *Drosophila* growth. *Cell* **114**, 739–749 (2003).
65. C. Géminard, E. J. Rulifson, P. Léopold, Remote control of insulin secretion by fat cells in *Drosophila*. *Cell Metab.* **10**, 199–207 (2009).
66. R. Sousa-Nunes, L. L. Yee, A. P. Gould, Fat cells reactivate quiescent neuroblasts via TOR and glial insulin relays in *Drosophila*. *Nature* **471**, 508–512 (2011).
67. A. Rajan, N. Perrimon, *Drosophila* cytokine unpaired 2 regulates physiological homeostasis by remotely controlling insulin secretion. *Cell* **151**, 123–137 (2012).
68. H. Sano, Coupling of growth to nutritional status: The role of novel periphery-to-brain signaling by the CCh α 2 peptide in *Drosophila melanogaster*. *Fly (Austin)* **9**, 183–187 (2015).
69. A. F. Shamji, P. Nghiemi, S. L. Schreiber, Integration of growth factor and nutrient signaling: Implications for cancer biology. *Mol. Cell* **12**, 271–280 (2003).
70. M. Slaidina, R. Delanoue, S. Gronke, L. Partridge, P. Léopold, A *Drosophila* insulin-like peptide promotes growth during nonfeeding states. *Dev. Cell* **17**, 874–884 (2009).
71. D. Muramatsu, T. Kinjoh, T. Shinoda, K. Hiruma, The role of 20-hydroxyecdysone and juvenile hormone in pupal commitment of the epidermis of the silkworm, *Bombyx mori*. *Mech. Dev.* **125**, 411–420 (2008).
72. M. Bate, A. M. Arias, *The Development of Drosophila melanogaster* (Cold Spring Harbor Laboratory Press, 1993), vol. 1.
73. E. B. Dubrovsky, Hormonal cross talk in insect development. *Trends Endocrinol. Metab.* **16**, 6–11 (2005).